The EMBO Journal (2010) 29, 2888–2898 | © 2010 European Molecular Biology Organization | All Rights Reserved 0261-4189/10
www.embojournal.org

THE EMBO JOURNAL

Regulation of mitochondrial phospholipids by Ups1/PRELI-like proteins depends on proteolysis and Mdm35

Christoph Potting[1,2,3], Claudia Wilmes[1,3], Tanja Engmann[1], Christof Osman[1] and Thomas Langer[1,2,*]

[1]Institute for Genetics, Center for Molecular Medicine (CMMC), Cologne Excellence Cluster on Cellular Stress Responses in Aging-Associated Diseases (CECAD), University of Cologne, Cologne, Germany and [2]Max-Planck-Institute for Biology of Aging, Cologne, Germany

The mitochondrial phospholipid metabolism critically depends on members of the conserved Ups1/PRELI-like protein family in the intermembrane space. Ups1 and Ups2 (also termed Gep1) were shown to regulate the accumulation of cardiolipin (CL) and phosphatidylethanolamine (PE), respectively, in a lipid-specific but coordinated manner. It remained enigmatic, however, how the relative abundance of both phospholipids in mitochondrial membranes is adjusted on the molecular level. Here, we describe a novel regulatory circuit determining the accumulation of Ups1 and Ups2 in the intermembrane space. Ups1 and Ups2 are intrinsically unstable proteins, which are degraded by distinct mitochondrial peptidases. The turnover of Ups2 is mediated by the *i*-AAA protease Yme1, whereas Ups1 is degraded by both Yme1 and the metallopeptidase Atp23. We identified Mdm35, a member of the twin Cx_9C protein family, as a novel interaction partner of Ups1 and Ups2. Binding to Mdm35 ensures import and protects both proteins against proteolysis. Homologues to all components of this pathway are present in higher eukaryotes, suggesting that the regulation of mitochondrial CL and PE levels is conserved in evolution.

The EMBO Journal (2010) **29,** 2888–2898. doi:10.1038/emboj.2010.169; Published online 23 July 2010
Subject Categories: membranes & transport; proteins
Keywords: cardiolipin; intermembrane space; mitochondria; phospholipid; proteolysis

Introduction

Mitochondria are dynamic organelles, whose membranes constantly fuse and divide (Hoppins *et al*, 2007). The remodelling of the mitochondrial network makes it necessary to continuously adjust the supply of mitochondrial proteins and membrane lipids to meet specific physiological demands. Although the biogenesis of mitochondrial proteins has been extensively studied (Chacinska *et al*, 2009), little is known about how the accumulation of phospholipids in mitochondria is regulated. Some phospholipids, namely phosphatidylethanolamine (PE) and cardiolipin (CL), are synthesized within mitochondria from precursor forms first generated in the endoplasmatic reticulum (ER). One such precursor, phosphatidylserine (PS), is imported from the ER to the mitochondrial inner membrane, where it is subsequently decarboxylated to yield PE (Trotter *et al*, 1993; Gaigg *et al*, 1995). CL, a dimeric phosphoglycerolipid unique to the membranes of bacteria and mitochondria, is synthesized from phosphatidic acid through an enzymatic cascade in the inner membrane (Houtkooper and Vaz, 2008; Schlame and Ren, 2009).

The maintenance of a defined lipid composition of mitochondrial membranes is critical for their functionality and plasticity. CL, for instance, binds to many mitochondrial membrane proteins and is required for their optimal activities (Hoffmann *et al*, 1994; Lange *et al*, 2001; Shinzawa-Itoh *et al*, 2007; Claypool *et al*, 2008). Consequently, impaired accumulation of CL can result in defects of some mitochondrial functions, including the activity of respiratory chain complexes and of the F_1F_O ATP synthase, the stability of protein translocases and protein import, mitochondrial genome stability, mitochondrial fusion and the activation of apoptotic pathways (Zhong *et al*, 2004; Choi *et al*, 2007; DeVay *et al*, 2009; Gebert *et al*, 2009; Wenz *et al*, 2009; Wittig and Schägger, 2009). In humans, disturbances in the CL metabolism because of mutations in the mitochondrial transacylase tafazzin are associated with cardiomyopathy in Barth syndrome (Bione *et al*, 1996; Schlame and Ren, 2006; Houtkooper *et al*, 2009).

Increasing evidence suggests that not only the concentration of phospholipids but also their lateral distribution within the membrane can affect mitochondrial activities. Prohibitins, which assemble into large ring-shaped protein complexes in the inner membrane, have been proposed to act as membrane scaffolds that may affect the distribution of both proteins and phospholipids in the inner membrane (Tatsuta *et al*, 2005; Osman *et al*, 2009a, b). Prohibitin function has been linked to diverse processes in mitochondria, including mitochondrial fusion, the maintenance of cristae morphology, the stability of the mitochondrial genome and apoptotic processes (Bogenhagen *et al*, 2003; Kasashima *et al*, 2008; Merkwirth *et al*, 2008). The genetic interactome of prohibitins in yeast points to an intimate functional relationship to mitochondrial PE and CL metabolism, as mutations in central components of the biosynthetic pathways of PE and CL are synthetically lethal with prohibitins (Osman *et al*, 2009a). This suggests that lowered levels of these non-bilayer phospholipids are deleterious for cell survival in the absence of prohibitins.

These studies linked the function of a number of previously uncharacterized genes to the mitochondrial PE and

*Corresponding author. Institut für Genetik, Universität zu Köln, Zülpicher Strasse 47, 50674 Köln, Germany. Tel.: +49 221 470 4876; Fax: +49 221 470 6749; E-mail: thomas.langer@uni-koeln.de
[3]These authors contributed equally to this work

Received: 3 May 2010; accepted: 29 June 2010; published online: 23 July 2010

CL metabolism. These include members of a conserved family of Ups1/PRELI-like proteins in the intermembrane space, which harbour an ~170 amino acid long PRELI/MSF′ domain of unknown function (Dee and Moffat, 2005). Three representatives of this protein family are present in yeast: Ups1, Ups2 (also termed Gep1) and Ups3 (Gep2). Ups1 was originally identified to affect the processing of the dynamin-like GTPase Mgm1, a central component of the mitochondrial fusion machinery, and thereby mitochondrial shape (Sesaki *et al*, 2006). Ups1 and Ups2 were later found to regulate the accumulation of PE and CL in mitochondria (Tamura *et al*, 2009; Osman *et al*, 2009a). Ups1 is required to maintain normal CL levels, whereas PE levels are decreased in the absence of Ups2. Notably, the accumulation of PE and CL, both non-bilayer phospholipids with related biophysical properties, is coordinated and appears to depend critically on the relative abundance of Ups1 and Ups2 in the intermembrane space. Normal levels of CL were restored in Δ*ups1* cells lacking Ups2, whereas overexpression of Ups2 in wild-type cells reduced CL levels, suggesting a competition between Ups1 and Ups2 (Osman *et al*, 2009a).

Here, we have identified the twin Cx_9C protein Mdm35 as a novel-binding partner of both Ups1 and Ups2. Mdm35 ensures the efficient accumulation of Ups1 and Ups2 in mitochondria and protects these intrinsically unstable proteins against degradation by the *i*-AAA protease Yme1 and Atp23. Mitochondrial PE and CL levels are thus controlled and coordinated by a complex regulatory network built up of conserved proteins in the intermembrane space.

Results

Ups1 and Ups2 assemble with Mdm35 in the intermembrane space

Ups1 and Ups2 have previously been suggested to competitively regulate the levels of CL and PE in mitochondria (Osman *et al*, 2009a). To identify binding partners of both proteins, we generated yeast strains expressing genomically MYC-tagged Ups1 ($Ups1^{MYC}$) and Ups2 ($Ups2^{MYC}$) under the control of galactose-inducible promoters. $Ups1^{MYC}$ and $Ups2^{MYC}$ are functionally active and maintained normal cell growth and mitochondrial phospholipid levels (data not shown; Supplementary Figure S1). Mitochondria were isolated from $Ups1^{MYC}$- and $Ups2^{MYC}$-overexpressing cells, solubilized and extracts subjected to immunoprecipitation using MYC-specific antibodies (Figure 1A). Strikingly, a protein with a molecular mass of ~10 kDa that was identified as Mdm35 by peptide mass finger printing was co-purified with both $Ups1^{MYC}$ and $Ups2^{MYC}$ (Figure 1A). Mdm35 was not detected in immunoprecipitates when extracts of wild-type mitochondria lacking MYC-tagged Ups1 or Ups2 variants were analysed, demonstrating a specific interaction (Figure 1A).

To exclude that the overexpression of $Ups1^{MYC}$ and $Ups2^{MYC}$ induces artificial binding of Mdm35, we modified *UPS1* and *UPS2* genes by homologous recombination in such a way that variants harbouring C-terminal tandem affinity purification tags (TAP) were expressed genomically under the control of the endogenous promoter. Mitochondria were isolated from these cells, solubilized in detergent and the binding of $Ups1^{TAP}$ and $Ups2^{TAP}$ to Mdm35 was assessed by affinity chromatography (Figure 1B and C). Analysis of eluate fractions by immunoblotting revealed that Mdm35 interacts with both $Ups1^{TAP}$ and $Ups2^{TAP}$. When extracts with untagged Ups1 or Ups2 were applied, Mdm35 was not found in the bound fractions. Similarly, porin, an abundant mitochondrial outer membrane protein, was not detected in the eluate, further substantiating the specificity of the interaction between Mdm35 and both Ups1 and Ups2.

Hence, we conclude that Mdm35 assembles with Ups1 and Ups2 in the mitochondrial intermembrane space. Notably, we did not observe co-purification of Ups2 with tagged variants of Ups1 nor of Ups1 with tagged variants of Ups2. Moreover, deletion of *UPS1* did not affect the native molecular mass of

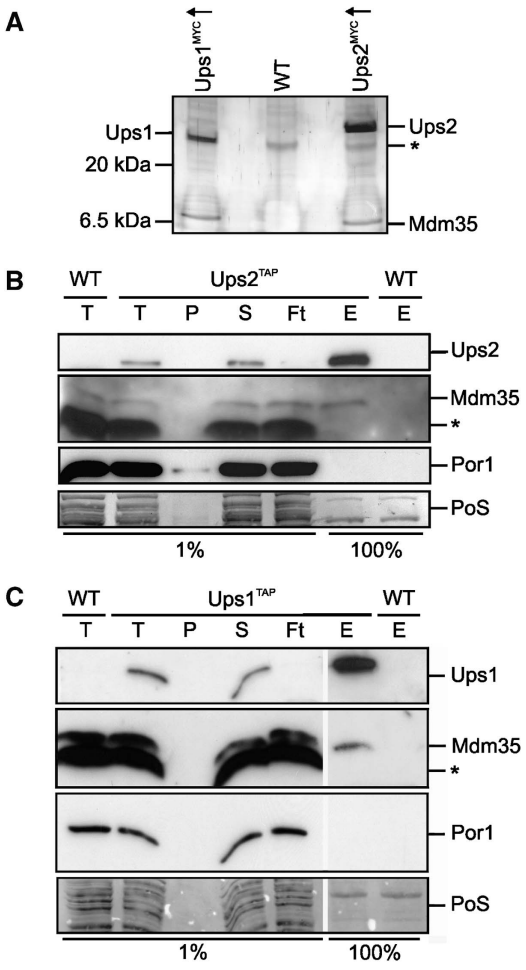

Figure 1 Mdm35 interacts with Ups1 and Ups2. (**A**) Coimmunoprecipitation of Mdm35 with $Ups1^{MYC}$and $Ups2^{MYC}$. Mitochondria isolated from wild-type cells (WT, CG214) or cells overexpressing either $Ups1^{MYC}$ ($Ups1^{MYC}$↑, CG630) or $Ups2^{MYC}$ ($Ups2^{MYC}$↑, CG626) were solubilized and subjected to coimmunoprecipitation using MYC-specific antibodies. Eluates were analysed by Tris/Tricine SDS–PAGE and subsequent silver staining. Ups1, Ups2 and Mdm35 were identified by peptide mass finger printing. The asterisk (*) marks a protein binding unspecifically to the beads. (**B**, **C**) Affinity purification of Mdm35 with endogenous levels of $Ups1^{TAP}$ and $Ups2^{TAP}$. Mitochondria isolated from wild-type cells (WT,CG214) or cells expressing either (**B**) $Ups2^{TAP}$ (CG591) or (**C**) $Ups1^{TAP}$ (CG593) from the endogenous gene locus were solubilized and proteins were affinity purified using immunoglobulin G-coupled beads. Total (T), pellet (P), supernatant (S) flow-through (Ft) fractions (1%) and the eluate (E) fraction (100%) were analysed by Tris/Tricine SDS–PAGE, followed by Ponceau S staining (PoS) and immunoblotting. The asterisk (*) marks a protein band cross-reacting with Mdm35 antibodies.

Ups2 when assessed using size exclusion chromatography (Supplementary Figure S2). Thus, consistent with their lipid-specific roles, Ups1 and Ups2 do not interact, suggesting that Mdm35 can independently bind both proteins.

Loss of Mdm35 mimics phenotypes of Δups2 cells

Mdm35 was identified as an intermembrane space protein that is essential for the maintenance of a tubular mitochondrial morphology; however, the molecular function of Mdm35 remained enigmatic (Dimmer *et al*, 2002; Gabriel *et al*, 2007; Longen *et al*, 2009). We recently identified Mdm35, along with Ups1 and Ups2, in a genome-wide screen for genes required for the survival of cells lacking prohibitins, putative scaffolding proteins in the inner membrane (Osman *et al*, 2009b). To further elucidate the molecular basis of the genetic interaction of Mdm35 with prohibitins, we generated Δ*phb1*Δ*mdm35* cells expressing *PHB1* from a tetracycline-regulatable promoter (Δ*phb1*Δ*mdm35* [*PHB1*]). These cells grew normally on fermentable and non-fermentable carbon sources under non-repressing conditions. However, cell growth was inhibited when *PHB1* expression was shut-off by the addition of the tetracycline analogue doxycycline, confirming the synthetic lethal interaction of *PHB1* and *MDM35* (data not shown). Downregulation of Phb1 in the absence of Mdm35 was accompanied by the loss of inner membrane and matrix proteins, such as Mgm1, Cox2, Yme1 and Aco1. Conversely, proteins localized to the outer membrane or the intermembrane space, porin and Tim13, respectively, remained unaffected (Figure 2A). These observations can be explained by the loss of the membrane potential across the inner membrane upon downregulation of Phb1 in Δ*phb1*Δ*mdm35* [*PHB1*] cells (Figure 2B). The membrane potential, which is required for protein import across and into the inner membrane and thus essential for cell survival, was decreased in Δ*mdm35* cells and further ceased upon depletion of Phb1 from Δ*phb1*Δ*mdm35* [*PHB1*] cells (Figure 2B).

These findings are reminiscent of Ups2-deficient cells in which the mitochondrial membrane potential was also dissipated upon downregulation of Phb1 (Osman *et al*, 2009a). Moreover, both Δ*mdm35* and Δ*ups2* mitochondria exhibit reduced levels of PE, prompting us to examine functional similarities between both proteins. We first monitored the synthesis of PE by the PS decarboxylase Psd1 in the intermembrane space in Δ*mdm35* mitochondria (Figure 2C). The mitochondrial outer membrane was disrupted by osmotic swelling generating mitoplasts, which we incubated with the fluorescently labelled PS (NBD-PS). NBD-PS was converted to NBD-PE in wild-type and Δ*mdm35* mitochondria but not in Δ*psd1* mitochondria (Figure 2C; data not shown), demonstrating that Mdm35 is not required for the synthesis of PE by Psd1 within mitochondria. We observed a modest but statistically significant increase in the rate of PE synthesis as we have previously reported for Δ*ups2* mitochondria (Osman *et al*, 2009a). These findings suggest that, similar to Ups2, Mdm35 ensures PE accumulation by either inhibiting its export from mitochondria or by preventing its lipolytic degradation.

Deletion of *UPS2* in Δ*ups1* cells restored CL levels in mitochondria and cell growth, indicating a coordinated regulation of CL and PE (Osman *et al*, 2009a). As both Ups1 and Ups2 bind Mdm35, we deleted *MDM35* in wild-type, Δ*ups1* and Δ*ups2* cells. In agreement with previous findings, growth

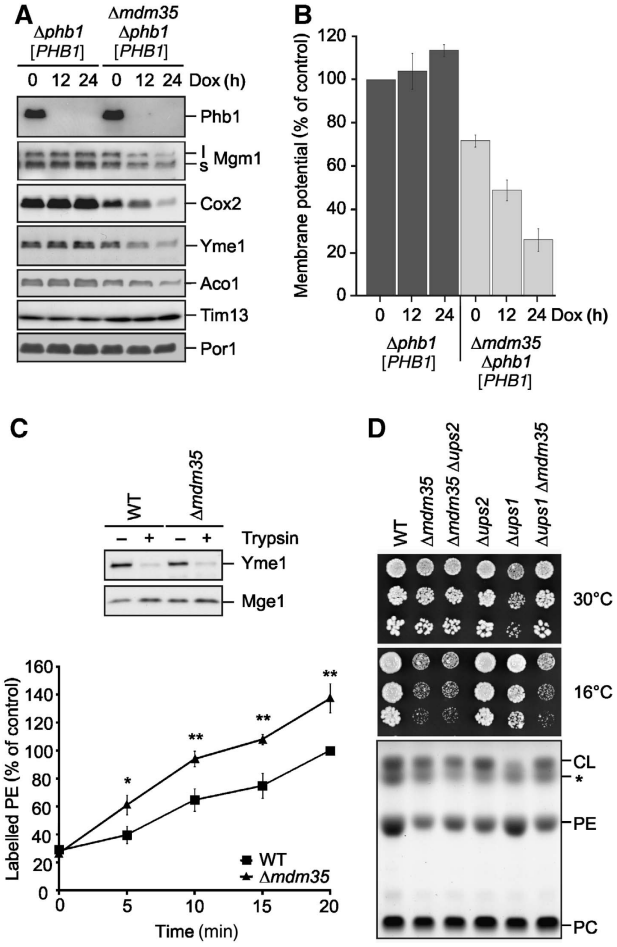

Figure 2 Phenotypic similarities between Mdm35- and Ups2-deficient cells. (**A**) Steady-state levels of mitochondrial proteins in Δ*mdm35*Δ*phb1* [*PHB1*] cells. Mitochondria were isolated from Δ*phb1* [*PHB1*] (CG278) and Δ*mdm35*Δ*phb1* [*PHB1*] (CG287) cells grown on galactose-containing media in the presence of doxycycline (Dox, 2 μg/ml) for the times indicated. Mitochondrial proteins were analysed by SDS–PAGE and immunoblotting. (**B**) Dissipation of the mitochondrial membrane potential in cells lacking Mdm35 and Phb1. Mitochondria were isolated from Δ*phb1* [*PHB1*] (CG278) and Δ*mdm35*Δ*phb1* [*PHB1*] (CG278) cells grown on galactose-containing media in the presence or absence of Dox for the indicated times. Membrane potential was measured using the membrane-potential sensitive dye 3,3′-dipropylthiadicarbocyanine iodide ($DiSC_3$ (5)). Data represent ± s.d. of three independent experiments. (**C**) Psd1 activity in the absence of Mdm35. Mitoplasts derived from wild-type (WT, CG1) or Δ*mdm35* (CG323) cells were generated by osmotic swelling. To monitor the disruption of the outer membrane, mitochondria were resuspended in SHKCl buffer (0.1 μg/μl) and subjected to trypsin treatment (0.25 μg/μl, 30 min, 4°C). Samples were further analysed by SDS–PAGE and immunoblotting using antibodies directed against the intermembrane space protein Yme1 and the matrix protein Mge1 (upper panel). Mitoplasts were incubated with NBD-PS for the indicated time periods. Phospholipids were separated by TLC and fluorescent NBD-PE was quantified by fluorescence imaging (lower panel). NBD-PE accumulating in wild-type (WT) mitochondria after 20 min was set to 100%. Data represent ± s.d. of three independent experiments. $^*P<0.05$, $^{**}P<0.005$. (**D**) Effects of *MDM35* deletion in Δ*ups1* cells. Five-fold serial dilutions of wild-type (WT, CG1), Δ*mdm35* (CG323), Δ*mdm35*Δ*ups2* (CW128), Δ*ups2* (CW130), Δ*ups1* (CW143), Δ*mdm35*Δ*ups1* (CW144) cells were spotted on YPD and incubated at the indicated temperature (upper panel). The mitochondrial lipid profile was analysed by TLC (lower panel). The asterisk (*) indicates an unidentified lipid species.

of Δ*mdm35* as well as Δ*ups2* cells on glucose-containing medium at 30°C was largely unaffected and mitochondrial PE levels were decreased (Figure 2D). Δ*mdm35*Δ*ups2* cells exhibited similar phenotypes (Figure 2D). Moreover, we noted a cold-sensitive phenotype of cells lacking Mdm35, regardless of the presence of Ups1 or Ups2 (Figure 2D). Ups1-deficient cells contained low CL levels in mitochondria and exhibited growth deficiencies on glucose-containing medium at 30°C (Figure 2D). Strikingly, deletion of *MDM35* restored normal CL levels in Δ*ups1* mitochondria and cell growth under these conditions (Figure 2D), substantiating the functional similarities between Ups2 and Mdm35.

Reduced steady-state levels of Ups2 in Δmdm35 cells

To further define the functional relationship of Mdm35 and Ups2, we genomically tagged Ups2 with a C-terminal MYC epitope in wild-type and Δ*mdm35* cells. Notably, $Ups2^{MYC}$ accumulated at reduced levels in these cells when *MDM35* was deleted (Figure 3A). Expression of plasmid-encoded *MDM35* restored the cold-sensitive growth phenotype of Δ*mdm35* cells and normal levels of $Ups2^{MYC}$ (Figure 3A).

The reduced steady-state concentration of Ups2 in the absence of Mdm35 could explain phenotypic similarities between Δ*mdm35* and Δ*ups2* cells. To investigate the possibility of a redundant function of both proteins, we overexpressed Ups2 in Δ*mdm35* cells and analysed the mitochondrial phospholipid profile (Figure 3B). However, overexpression of Ups2 did not restore PE levels in Δ*mdm35* mitochondria, although overexpressed Ups2 accumulated within mitochondria (Figure 3B). Thus, an increased expression of Ups2 does not substitute for loss of Mdm35 (Figure 3B). In contrast, we observed an impaired growth of Δ*mdm35* upon Ups2 overexpression, which only mildly affected the growth of wild-type cells under these conditions (Figure 3C). We have previously reported that overexpression of Ups2 decreases CL levels in mitochondria (Osman *et al*, 2009a) (Figure 3B). Similarly, CL accumulated at lower levels in Δ*mdm35* mitochondria if Ups2 was overexpressed (Figure 3B). It is thus conceivable that the severely impaired growth of Δ*mdm35* cells overexpressing Ups2 is caused by the combined effects of reduced CL and PE concentrations in mitochondrial membranes (Gohil *et al*, 2005).

Degradation of Ups2 by the i-AAA protease Yme1

The decreased steady-state concentration of $Ups2^{MYC}$ in Δ*mdm35* cells may result from an impaired expression or biogenesis of Ups2 in these cells or may reflect proteolytic turnover within mitochondria. To distinguish between these possibilities, we raised polyclonal antibodies directed against Ups2 and examined the accumulation of Ups2 in extracts of wild-type cells and cells lacking various mitochondrial peptidases (Figure 4A). We did not detect Ups2 in mitochondria-enriched membrane fractions of wild-type cells using affinity-purified antibodies, but observed the accumulation of a band at the expected molecular mass of Ups2 in a corresponding fraction of cells lacking Yme1, a subunit of the ATP-dependent *i*-AAA protease active in the mitochondrial intermembrane space (Figure 4A) (Leonhard *et al*, 1996; Weber *et al*, 1996). This band was not detected in extracts of cells lacking other mitochondrial proteases that function in the inner membrane or the intermembrane space (Figure 4A).

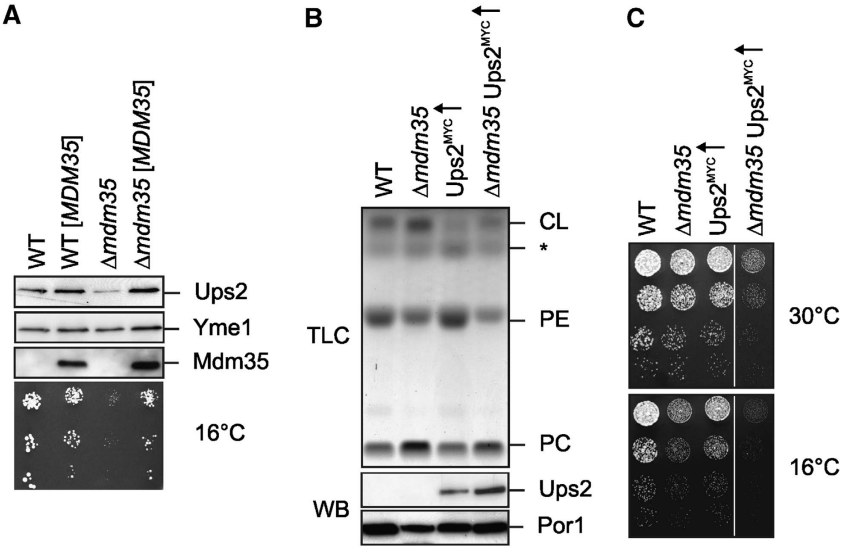

Figure 3 Mdm35 controls the accumulation of Ups2 in mitochondria. (**A**) Steady-state levels of $Ups2^{MYC}$ in cells containing different amounts of Mdm35. Wild-type (WT) and Δ*mdm35* cells expressing genomically tagged $Ups2^{MYC}$ were transformed with either YCplac111::ADH (PY127, PY129) or YCplac111::ADH encoding *MDM35* ([*MDM35*]) (PY128, PY130). Cells were grown to mid-log phase in selective synthetic glucose media. Proteins were extracted from mid-log phase cells by alkaline lysis, analysed by SDS–PAGE and immunoblotting using Yme1-, MYC- and affinity-purified Mdm35-specific antibodies (upper panel). Five-fold serial dilutions of these cells were spotted on selective, glucose-containing plates and incubated at 16°C (lower panel). (**B**, **C**) Ups2 overexpression does not restore normal PE levels and cell growth in the absence of Mdm35. (**B**) TLC analysis of mitochondrial lipids in wild-type (WT, CG214), Δ*mdm35* (CG524), $Ups2^{MYC}\uparrow$ (CG626) and Δ*mdm35* $Ups2^{MYC}\uparrow$ (PY64) cells (upper panel). The asterisk (*) indicates an unidentified lipid species. Mitochondria purified by sucrose-gradient centrifugation were used for determination of the phospholipid profile and were analysed by SDS–PAGE and immunoblotting using porin- (Por1) and MYC-specific antibodies (lower panel). (**C**) Five-fold serial dilutions of mid-log phase cultures of the cells were spotted on YP plates containing galactose and incubated at 16 or 30°C.

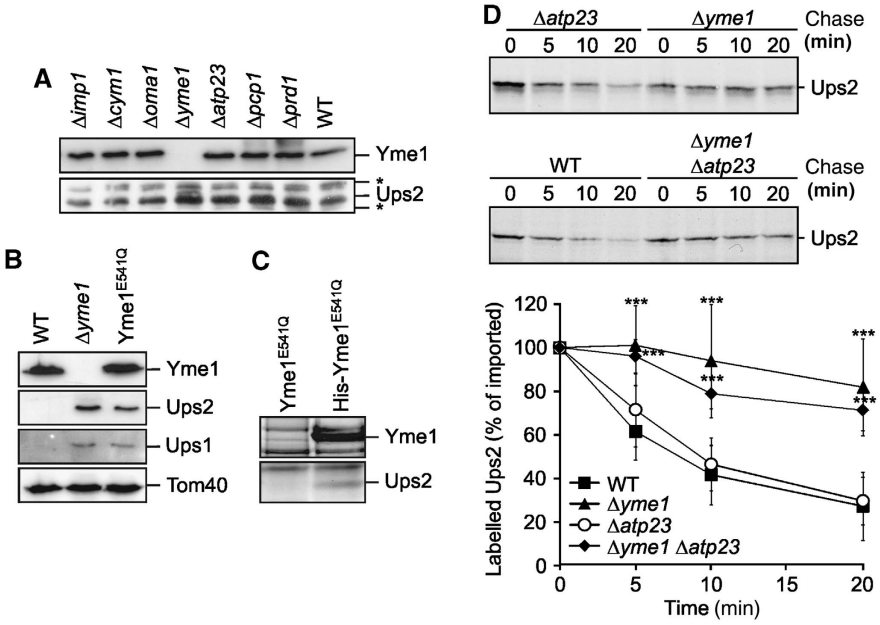

Figure 4 Ups2 is degraded by the *i*-AAA protease Yme1. (**A**) Accumulation of Ups2 in Δ*yme1* cells. Wild-type cells (WT, CG214) and cells lacking different mitochondrial peptidases [Δ*imp1* (Euroscarf 732), Δ*cym1* (Euroscarf 4266), Δ*oma1* (Euroscarf 6003), Δ*yme1*(CG113), Δ*atp23* (CW1), Δ*pcp1* (Euroscarf 4731), Δ*prd1*(Euroscarf 3464)] were grown to mid-log phase on glucose-containing media. Mitochondria-enriched membrane fractions were analysed by SDS–PAGE and immunoblotting using Yme1- and affinity-purified Ups2-specific antibodies. Asterisks (*) indicate protein bands cross-reacting with the Ups2-antibodies. (**B**) Ups1 and Ups2 accumulate in mitochondria lacking proteolytically active Yme1. Mitochondria isolated from wild-type cells (WT, CG1), Δ*yme1*(VIA4) cells or Δ*yme1* cells expressing proteolytically inactive Yme1^{E541Q} (YTE26) were analysed by SDS–PAGE and immunoblotting using Yme1-, Tom40- and affinity-purified Ups1- and Ups2-specific antibodies. (**C**) Binding of Ups2 to proteolytically inactive Yme1^{E541Q}. Mitochondria isolated from *yme1* cells expressing either Yme1^{E541Q} (YTE26) or a variant thereof carrying an N-terminal hexahistidine tag (His Yme1^{E541Q}) (YTE89) were solubilized and extracts subjected to Ni-NTA affinity chromatography. Eluate fractions were analysed by SDS–PAGE and Coomassie staining. Ups2 was detected by peptide mass finger printing in the eluate only when mitochondria harbouring His-Yme1^{E541Q} were analysed. (**D**) Degradation of Ups2 by Yme1 following import into mitochondria *in vitro*. Radiolabelled Ups2 was imported into mitochondria derived from either wild-type (WT, CG1), Δ*yme1* (VIA4), Δ*atp23* (CW3) or Δ*yme1*Δ*atp23* (CW79) cells. The stability of newly imported Ups2 upon further incubation at 37°C was assessed by SDS–PAGE and autoradiography. Quantification of Ups2 accumulation in mitochondria is represented in the lower panel. Newly imported Ups2 was set to 100%. Data represent ± s.d. of four independent experiments. $***P<0.0005$.

We purified mitochondria from wild-type cells, Δ*yme1* cells and Δ*yme1* cells expressing proteolytically inactive Yme1, which harbours a mutation in the proteolytic centre (Yme1^{E541Q}). Immunoblotting using Ups2-specific antibodies detected Ups2 in mitochondria isolated from Δ*yme1* and *yme1*^{E541Q} cells, but not in wild-type or Δ*yme1*Δ*ups2* mitochondria (Figure 4B; Supplementary Figure S3). Similarly, Ups1 accumulates in mitochondria lacking functionally active Yme1 but not in Δ*yme1*Δ*ups1* mitochondria (Figure 4B; Supplementary Figure S3; see below). These results confirm the specificity of the Ups2 and Ups1 antibodies and suggest degradation of Ups2 by the *i*-AAA protease Yme1 in mitochondria.

This conclusion was further supported by the identification of Ups2 as a binding partner of proteolytically inactive Yme1^{E541Q}. Yme1^{E541Q} and a variant thereof harbouring a hexahistidine peptide at the amino terminal end of the mature protein (His-Yme1^{E541Q}) were expressed in Δ*yme1* cells. Mitochondria were isolated from these cells, solubilized and the extracts subjected to Ni-NTA affinity chromatography (Figure 4C). Ups2 was specifically detected by mass peptide finger printing in the eluate when mitochondria-containing His-Yme1^{E541Q} were analysed (Figure 4C). In contrast, Ups2 did not co-purify with proteolytically inactive *i*-AAA protease complexes lacking the hexahistidine epitope, demonstrating the specificity of the interaction (Figure 4C).

The binding of Ups2 to proteolytically inactive Yme1^{E541Q} and the accumulation of Ups2 in *yme1*^{E541Q} cells *in vivo* strongly suggests that Ups2 is a proteolytic substrate of Yme1. To directly monitor Yme1-dependent degradation of Ups2, we assessed the stability of Ups2 after import into isolated mitochondria. Ups2 was synthesized in a cell-free system in the presence of ^{35}S-methionine and imported posttranslationally into mitochondria isolated from wild-type and Δ*yme1* cells (Figure 4D). As a control, we also monitored the stability of newly imported Ups2 in mitochondria lacking the metallopeptidase Atp23 in the intermembrane space (Figure 4D). We observed that newly imported Ups2 was rapidly degraded in wild-type and Δ*atp23* mitochondria, but accumulated in Δ*yme1* and Δ*yme1*Δ*atp23* mitochondria, consistent with an Yme1-dependent proteolysis of Ups2 in the intermembrane space (Figure 4D). Taken together, these experiments identify Ups2 as a novel substrate of the *i*-AAA protease Yme1 in mitochondria.

Accumulation of Ups2 in mitochondria depends on Mdm35

To examine whether Yme1-dependent degradation explains the decreased accumulation of Ups2 in Δ*mdm35* mitochondria, we generated Δ*yme1*Δ*mdm35* cells by mating haploid Δ*yme1* and Δ*mdm35* cells followed by sporulation and tetrad dissection. The growth of double-mutant spores lacking

YME1 and *MDM35* was severely impaired (Figure 5A). Notably, we observed a synthetic lethal interaction of both genes when mutations were introduced in an S288c rather than a W303 strain background (Figure 5A).

We reasoned that an impaired accumulation of phospholipids could be responsible for the impaired cell growth and therefore analysed the phospholipid profile of Δ*yme1*Δ*mdm35* mitochondria in a W303 strain background by thin layer chromatography (TLC; Figure 5B). Both PE and CL failed to reach levels found in wild-type mitochondria. Moreover, the phospholipid profile was strikingly similar to that of Δ*mdm35* cells overexpressing Ups2 (Figure 3B). It is therefore conceivable that the impaired degradation of Ups2 causes the decreased PE and CL levels in Δ*yme1*Δ*mdm35* cells.

Indeed, immunoblotting of mitochondrial extracts using Ups2-specific antibodies revealed an increased steady-state amount of Ups2 in Δ*yme1*Δ*mdm35* mitochondria when compared with wild-type or Δ*mdm35* mitochondria (Figure 5C), indicating that Ups2 is degraded by the *i*-AAA protease in the absence of Mdm35. However, Ups2 accumulated at lower levels in Δ*yme1*Δ*mdm35* mitochondria than in Δ*yme1* cells (Figure 5C). It therefore appears that Mdm35 not only protects Ups2 against degradation by Yme1 but also ensures the efficient accumulation of Ups2 in mitochondria.

To address if Mdm35 affects the import of newly synthesized Ups2 into mitochondria, Ups2 was translated in a cell-free system in the presence of ^{35}S-methionine and imported into mitochondria isolated from wild-type cells, Δ*mdm35* cells and wild-type cells overexpressing Mdm35 (Figure 5D). ^{35}S-labelled Ups2 accumulated in mitochondria in a membrane-potential independent manner (data not shown). Its import was severely impaired into mitochondria isolated from Δ*mdm35* cells, whereas overexpression did not alter the rate of Ups2 import (Figure 5D). In contrast, import of the intermembrane space protein Tim9 was not altered in the absence or upon overexpression of Mdm35 (Figure 5D). These results indicate that Mdm35 affects but is not rate limiting for import.

Ups2 accumulated within Δ*mdm35*Δ*yme1* mitochondria, demonstrating that Mdm35 is not essential for the import of Ups2 *in vivo* (Figure 5C). On the other hand, import of ^{35}S-labelled Ups2 into isolated Δ*mdm35* mitochondria lacking Yme1 was not restored to wild-type levels, suggesting that efficient Ups2 import depends on Mdm35 (Supplementary Figure S4). It should be noted, however, that the integrity of Δ*mdm35*Δ*yme1* mitochondria appears to be severely compromised. Consistent with the described growth deficiencies (Figure 5A), the membrane potential across the inner membrane and import of a matrix-targeted protein into mitochondria were impaired (Supplementary Figure S4). It therefore remains to be determined, whether the apparent requirement of Mdm35 for the import of Ups2 reflects a specific function of Mdm35 or an indirect effect of the aberrant phospholipid composition of mitochondria lacking both Yme1 and Mdm35 (see Figure 5B).

Mdm35 protects Ups1 against degradation by Yme1 and Atp23

As Mdm35 binds both Ups1 and Ups2, we monitored the accumulation of Ups1 in Δ*mdm35* cells in further experiments. The *UPS1* gene was genomically modified in wild-type and Δ*mdm35* cells, allowing the expression of an

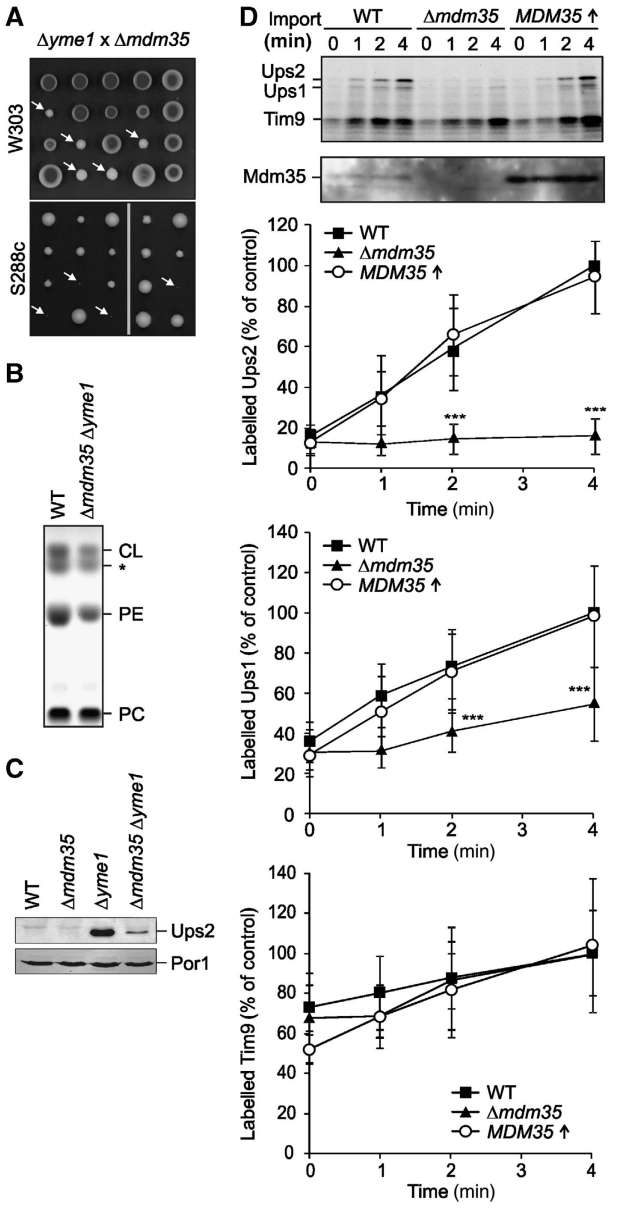

Figure 5 Mdm35 controls cell growth and the lipid composition of mitochondrial membranes in an Yme1-dependent manner. (**A**) Genetic interaction of *MDM35* and *YME1*. Diploid Δ*mdm35*Δ*yme1* cells that were obtained by mating of Δ*mdm35* and Δ*yme1* cells (CG324 × VIA5, CG560 × CG113) were sporulated and meiotic spores were grown on glucose-containing medium. White arrows indicate double-mutant progenies in the W303 strain background or inviable double-mutant spores in the strain S288c. (**B**) Reduced PE and CL levels in Δ*mdm35*Δ*yme1* mitochondria. Phospholipid profiles of wild-type (WT, CG1) and Δ*yme1*Δ*mdm35* (CW414) mitochondria were analysed by TLC. The asterisk (*) indicates an unidentified lipid species. (**C**) Ups2 accumulates in Δ*mdm35*Δ*yme1* cells. Mitochondria were isolated from wild-type (WT, CG1), Δ*mdm35* (CG323), Δ*yme1* (VIA4), and Δ*mdm35*Δ*yme1* (CW414) cells grown on galactose-containing media and analysed by Tris/Tricine gradient SDS–PAGE and immunoblotting using porin (Por1)- and affinity-purified Ups2-specific antibodies. (**D**) Accumulation of Ups2 in mitochondria upon import *in vitro* depends on Mdm35. Radiolabelled Ups1, Ups2 and, for control, Tim9, were imported into wild-type (WT, CG1), Δ*mdm35* (CG323) and Mdm35-overexpressing (CW343) mitochondria for the indicated time. The analysis of the samples by Tris/Tricine gradient SDS–PAGE and autoradiography is shown in the upper panels. A quantification of imported Ups1, Ups2 and Tim9 is shown in the lower panels. Protein imported into wild-type (WT) mitochondria after 4 min was set to 100%. Data represent ± standard deviation of six independent experiments. ***$P<0.0005$.

MYC-tagged variant from the endogenous promoter, as previously described for *UPS2*. Ups1 and Ups2 were detected in extracts of wild-type and Δ*mdm35* cells expressing $Ups1^{MYC}$ or $Ups2^{MYC}$ by immunoblotting using MYC-specific antibodies (Figure 6A). Interestingly, $Ups1^{MYC}$ accumulated in the cells at ~6-fold lower levels than $Ups2^{MYC}$ (Figure 6A). Similar to Ups2, Ups1 levels were decreased in the absence of Mdm35 (Figure 6A) and less $Ups1^{MYC}$ accumulated in a mitochondrial fraction isolated from Δ*mdm35* cells (Figure 6B). Mdm35 was not detectable in the wild-type fraction, but when overexpressed from a centromer-based plasmid restored levels of Ups1 in Δ*mdm35* cells (Figure 6B). These results indicate that Mdm35 may affect that stability of Ups1 and Ups2 in a similar manner.

We therefore examined the import of ^{35}S-labelled Ups1 into mitochondria isolated from wild-type cells, Δ*mdm35* cells and wild-type cells overexpressing Mdm35. Import of Ups1 was impaired in the absence of Mdm35, although to a lesser extent than we had observed for Ups2 (Figure 5D). Overexpression of Mdm35 did not affect the rate of Ups1 import into mitochondria (Figure 5D). Moreover, newly imported Ups1 was degraded similar to Ups2 (Figure 6C).

Surprisingly, deletion of *YME1* caused only a minor, but statistically significant stabilization of newly imported Ups1, indicating that another peptidase may mediate proteolysis of Ups1 in Δ*yme1* mitochondria (Figure 6C). We therefore examined the stability of Ups1 in mitochondria lacking other mitochondrial peptidases. A decreased rate of

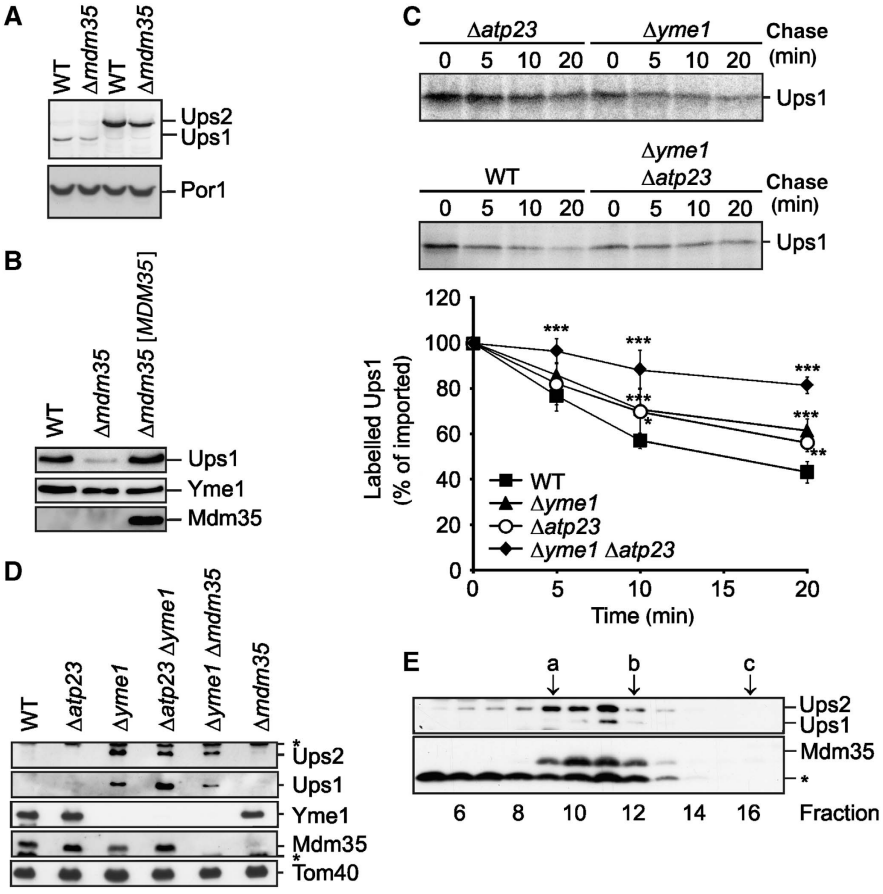

Figure 6 Mdm35 controls degradation of Ups1 by Yme1 and Atp23. (**A**) Ups1 is less abundant than Ups2. Wild-type (WT) and Δ*mdm35* cells expressing genomically tagged $Ups2^{MYC}$ (PY102, PY117) or $Ups1^{MYC}$ (PY103, CW385) were grown to mid-log phase. Proteins were extracted and analysed by SDS–PAGE and immunoblotting using MYC- and porin (Por1)-specific antibodies. (**B**) Steady-state levels of $Ups1^{MYC}$ in the absence of Mdm35. Wild-type (WT) and Δ*mdm35* cells expressing genomically modified $Ups1^{MYC}$ were transformed with either YCplac111::ADH (CW394, CW398) or YCplac111::ADH encoding *MDM35* ([*MDM35*]) (CW396). Mitochondria-enriched membrane fractions were analysed by SDS–PAGE and immunoblotting using MYC-, Yme1- and affinity-purified Mdm35-specific antisera. (**C**) Ups1 is stabilized in mitochondria lacking *YME1* and *ATP23*. Radiolabelled Ups1 was imported into mitochondria isolated from WT (CG1), Δ*yme1* (VIA4), Δ*atp23* (CW3) or Δ*yme1*Δ*atp23* (CW79) cells and the stability of newly imported Ups1 upon further incubation at 37°C was assessed by SDS–PAGE and autoradiography. Quantification of Ups1 accumulation in mitochondria is shown in the lower panel. Newly imported Ups1 was set to 100%. Data represent ±s.d. of four independent experiments. $*P<0.05$, $**P<0.005$, $***P<0.0005$. (**D**) Steady-state levels of Ups1 and Ups2 in mitochondria lacking Yme1 and Atp23. Mitochondria were isolated from WT (CG), Δ*atp23* (CW3), Δ*yme1* (VIA4), Δ*atp23*Δ*yme1* (CW79), Δ*yme1*Δ*mdm35* (CW414) and Δ*mdm35* (CG323) cells and analysed by SDS–PAGE and immunoblotting using Yme1-, Tom40- and affinity-purified Mdm35-, Ups1- and Ups2-specific antibodies. (**E**) Quantitative assembly of Ups1 and Ups2 with Mdm35 in Δ*yme1* mitochondria. Sucrose-gradient purified mitochondria isolated from Δ*yme1* cells were solubilized in 1% (w/v) dodecylmaltoside (DDM) at a protein concentration of 5 mg/ml. After a clarifying spin, extracts were subjected to sizing chromatography using a Superose 12 column (GE Healthcare), which had been equilibrated with 0.1% (w/v) DDM, 25 mM Tris/HCl pH 7.4, 150 mM NaCl, 10% (v/v) glycerol. Eluate fractions were TCA-precipitated and analysed by gradient Tris/Tricine gradient SDS–PAGE and immunoblotting using Ups1-, Ups2- and Mdm35-specific antisera. (a) alcoholdehydrogenase (150 kDa), (b) ovalbumine (44.3 kDa), (c) cytochrome c (12.4 kDa). The asterisk (*) refers to a band unspecifically cross-reacting with the respective antiserum (**D**, **E**).

proteolysis was observed when Ups1 was imported in Δ*atp23* mitochondria, suggesting that Yme1 and Atp23 may exert overlapping functions and affect the stability of Ups1 (Figure 6C). To directly assess this possibility, we generated Δ*yme1*Δ*atp23* cells and examined the stability of Ups1 after import into isolated mitochondria (Figure 6C). Newly imported Ups1 was stabilized in Δ*yme1*Δ*atp23* to a greater extent than in either single mutant, indicating that both Yme1 and Atp23 can mediate the proteolytic turnover of Ups1.

We raised polyclonal antibodies directed against Ups1 to monitor the stability of Ups1 *in vivo*. Ups1 was not detectable using affinity-purified antibodies when mitochondria were isolated from wild-type cells (Figure 6D). In contrast, Ups1 accumulated in Δ*yme1* mitochondria or mitochondria harbouring proteolytically inactive Yme1^{E541Q} (Figures 4B and 6D; Supplementary Figure S3). Similar to Ups2, we observed a decreased steady-state concentration of Ups1 in Δ*yme1*Δ*mdm35* mitochondria when compared with Δ*yme1* mitochondria, which is consistent with the decreased import of Ups1 in the absence of Mdm35 (Figure 6D). Deletion of *ATP23* resulted in a further accumulation of Ups1 in Δ*yme1* cells (Figure 6D). This is in contrast to Ups2, which accumulated at similar levels in Δ*yme1* and Δ*yme1*Δ*atp23* mitochondria (Figure 6D). These results substantiate our *in vitro* mitochondrial import experiments and suggest that Atp23 affects Ups1 specifically. We therefore conclude that Ups2 is degraded by Yme1, whereas the steady-state concentration of Ups1 is regulated by both Yme1 and Atp23.

The accumulation of Ups1 and Ups2 in Δ*yme1* mitochondria allows detection of both proteins by immunoblotting and therefore enabled us to assess their assembly with Mdm35 *in vivo*. Mitochondria were isolated from Δ*yme1* cells, solubilized in dodecylmaltoside and extracts were analysed by size exclusion chromatography (Figure 6E). Ups1 and at least part of Ups2 co-eluted with Mdm35 from the column in fractions corresponding to an apparent molecular mass of ~60 kDa. Thus, both proteins assemble quantitatively with Mdm35 into stable complexes in the intermembrane space.

Discussion

Our experiments reveal an intriguing regulatory network in the mitochondrial intermembrane space, which coordinates the accumulation of CL and PE in mitochondria (Figure 7). Ups1 and Ups2 act as central regulators and affect specifically CL and PE, respectively. We demonstrate that both proteins associate with Mdm35, a conserved member of the twin Cx_9C protein family (Dimmer *et al*, 2002; Gabriel *et al*, 2007; Longen *et al*, 2009), which determines the accumulation of Ups1 and Ups2 within mitochondria. Mdm35 ensures efficient import and protects both proteins against proteolytic degradation in the intermembrane space. Whereas Ups2 is degraded by the *i*-AAA protease Yme1, proteolysis of Ups1 can be mediated by both Yme1 and Atp23 (Figure 7). All components of this regulatory network have been previously demonstrated to genetically interact with prohibitins, putative scaffolding proteins in the inner membrane, suggesting that a defined membrane organization is crucial for the regulation of the mitochondrial phospholipid metabolism (Osman *et al*, 2009a). Moreover, as all components are evolutionary conserved, PE and CL levels in mitochondria are likely controlled by a similar regulatory network in higher eukaryotes.

Mdm35 takes centre stage in this pathway as it binds both Ups1 and Ups2. Deletion of *MDM35* causes similar deficiencies as exhibited by Δ*ups2* cells and results in decreased PE levels in mitochondria. These include mitochondrial morphology defects observed in the absence of Mdm35 or Ups2 (Dimmer *et al*, 2002; Tamura *et al*, 2009; Osman *et al*, 2009a). The phenotypic similarities between Δ*mdm35* and Δ*ups2* cells indicate that defects in mitochondrial morphology in these cells are indeed caused by deficiencies in the phospholipid metabolism. CL levels, on the other hand, are

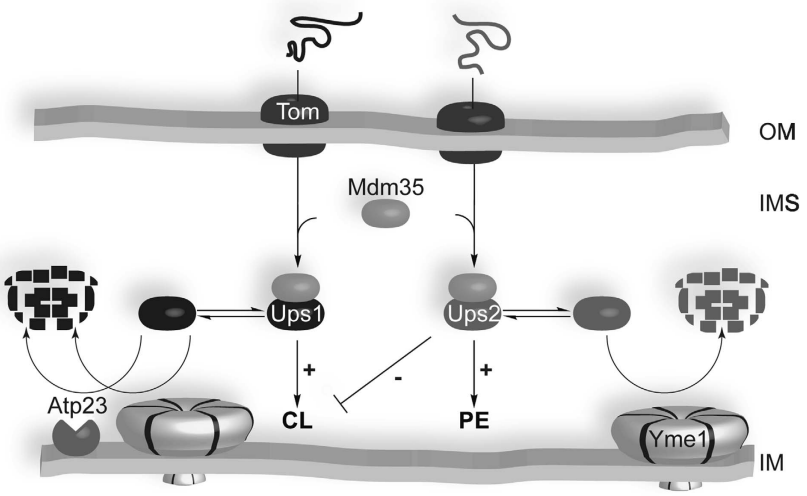

Figure 7 A conserved regulatory pathway determines the accumulation of Ups1 and Ups2 in the intermembrane space, which regulate the phospholipid composition of mitochondrial membranes. Ups1 and Ups2 are unstable proteins that are degraded by the *i*-AAA protease Yme1 and in the case of Ups1, also by Atp23. Binding of Mdm35 stabilizes Ups1 and Ups2 against proteolysis and ensures accumulation of both proteins in the intermembrane space. Both Ups1 and Ups2 have been found to be membrane associated (Tamura *et al*, 2009; Osman *et al*, 2009a) but are shown as soluble proteins in the IMS for simplicity. See text for details. IM, mitochondrial inner membrane; IMS, mitochondrial intermembrane space; OM, mitochondrial outer membrane.

much less affected than PE levels upon deletion of *MDM35*. The phospholipid composition of mitochondrial membranes in Δ*mdm35* cells is thus similar to that in Δ*ups1*Δ*ups2* cells, which suggests that the complex of Mdm35 with Ups1/PRELI-like proteins represents the physiologically active structure. Deletion of *MDM35* restores CL levels in Δ*ups1* mitochondria, as observed for a deletion of *UPS2* (Tamura *et al*, 2009; Osman *et al*, 2009a), consistent with a competition of Ups1/Mdm35 and Ups2/Mdm35 complexes. Interestingly, Δ*mdm35* cells cannot tolerate an accumulation of Ups2 in mitochondria, either upon ectopic overexpression or upon deletion of *YME1*. Accordingly, Ups2 may also function independently of Mdm35 or overexpression of Ups2 saturates yet another component that can substitute at least to some extent for functions of Mdm35. Regardless, Ups2 overexpression decreases CL levels and severely impairs cell growth, illustrating that a fine-tuned accumulation of CL and PE is pivotal for cell survival.

How does Mdm35 affect the mitochondrial phospholipid metabolism? Mdm35 protects Ups1 and Ups2 against proteolysis, which both accumulate at reduced levels in Δ*mdm35* mitochondria. Ups1 and Ups2 are intrinsically unstable proteins that undergo constant proteolysis even under normal growth conditions in wild-type cells. We propose that both proteins are stabilized in a folded state upon binding to Mdm35. Such a mechanism would allow to adjusting quickly the activity of Ups1 and Ups2 to specific physiological demands. It is an exciting possibility but remains to be verified experimentally that the function of Mdm35 is affected under stress conditions. As discussed for other Cx_9C protein family members (Riemer *et al*, 2009), oxidative stress or altered redox conditions in the intermembrane space might affect the function of Mdm35, and thereby impact on the mitochondrial phospholipid metabolism. Additional components are likely to be involved in this regulatory circuit, which could explain why Ups1 or Ups2 did not accumulate if only Mdm35 is overexpressed.

The *i*-AAA protease Yme1 regulates the stability of both Ups1 and Ups2. We observed increased steady-state concentrations of both proteins in mitochondria lacking Yme1 or harbouring the proteolytically inactive variant $Yme1^{E541Q}$. The *i*-AAA protease has been demonstrated to mediate the proteolysis of non-assembled or misfolded inner membrane proteins (Leonhard *et al*, 2000). Ups1 and Ups2 represent the first substrate proteins that are degraded even under physiological conditions by Yme1. Yme1-mediated proteolysis is not affected in the absence of the Mgr1/Mgr3 complex (CP and TL, unpublished data) that has been proposed to act as a substrate adaptor (Dunn *et al*, 2008). It is therefore likely that the *i*-AAA protease recognizes the folding state of Ups1 and Ups2 by virtue of its chaperone-like activity. In contrast to Ups2, turnover of Ups1 can also be mediated by Atp23, a conserved metallopeptidase in the mitochondrial intermembrane space. Atp23 mediates the maturation of mitochondrially encoded F_1F_O-ATP synthase subunit 6 (Atp6) in yeast (Osman *et al*, 2007; Zeng *et al*, 2007). However, given that mammalian Atp6 is synthesized without cleavable presequence, other substrates of Atp23 must exist in mammalian mitochondria. Our experiments demonstrate that Atp23 does not only act as a processing peptidase in mitochondria but is capable to degrade Ups1. How the different activities of Atp23 are regulated remains to be determined. Substrate proteins appear to be recognized in a highly specific manner, as Atp23 regulates the stability of Ups1 but not that of Ups2, although both proteins share amino-acid sequence similarities and are apparently unfolded in the intermembrane space.

Turnover of Ups1 and Ups2 offers an additional possibility to regulate the accumulation of phospholipids in mitochondria to meet different physiological demands. Modestly, increased PE and CL levels have been observed in the absence of Yme1 in cells grown on glucose-containing media (Nebauer *et al*, 2007), consistent with Yme1 controlling the steady-state concentration of both Ups1 and Ups2. It remains to be determined whether deletion of *ATP23* affects mitochondrial phospholipids under these growth conditions, although Atp23 only degrades Ups1 that is present at lower levels than Ups2 in mitochondria.

Turnover of Ups1 and Ups2 alone seemingly cannot account for the reduced steady-state levels of Ups1 and Ups2 in the absence of Mdm35. Ups2 is protected against degradation and accumulates in Δ*mdm35* cells if Yme1 is absent, but Ups2 levels remain reduced relative to Δ*yme1* cells. We observed reduced import of Ups2 and, to a lesser extent, of Ups1 in mitochondria lacking Mdm35. It is thus possible that Mdm35 has two independent roles for import and stability of Ups1-like proteins. We favour, however, the possibility that deficiencies in the import and stability of Ups1-like proteins in Δ*mdm35* mitochondria are the consequence of one molecular function of Mdm35, namely binding to Ups1-like proteins. Complex formation has a dual effect: it stabilizes newly imported molecules against proteolysis and traps these molecules in the intermembrane space. This is reminiscent of other intermembrane space proteins, like cytochrome c heme lyase, whose permanent association with preexisting proteins drives their translocation across the outer membrane (Neupert and Herrmann, 2007). Similarly, complex formation with Mdm35, though not essential for import, appears to ensure the efficient accumulation of Ups1 and Ups2 in the intermembrane space.

Materials and methods

Yeast strains and growth conditions

Yeast strains used in this study are derivatives either of W303 or S288c (Brachmann *et al*, 1998) and are listed in Supplementary Table 1. Yeast cells were grown according to standard procedures (Sherman, 2002).

Isolation of mitochondria

Cells were grown on yeast peptone (YP) medium containing 2% (w/v) galactose and 0.5% (w/v) lactate to an OD of ~2. Crude mitochondria were obtained as described previously with minor modifications (Daum *et al*, 1982). For further purification, the crude mitochondrial fraction was subjected to centrifugation, the mitochondrial pellet was resuspended in buffer A (0.6 M sorbitol and 5 mM MES, pH 6) and loaded on a continuous sucrose gradient (20–50% in buffer A). Mitochondria were harvested from the lower third of the gradient and diluted 1:5 in buffer A, pelleted, washed once in SEM buffer (250 mM sucrose, 10 mM MOPS/KOH, pH 7.2, and 1 mM EDTA) and finally resuspended in SEM buffer.

Co-immunoprecipitation experiments

Purified mitochondria (10 mg of protein; CG214, CG626, CG630) were resuspended at 2 mg/ml in buffer B (0.5% (w/v) digitonin, 25 mM Tris/HCl pH 7.4, 150 mM NaCl, 10% glycerol) and solubilized for 30 min at 4°C. Following a clarifying spin for 15 min at 100 000*g* at 4°C, the supernatant was incubated with anti-MYC antibodies (Sigma) previously cross-linked to protein A sepharose (GE Healthcare CL-4B). Beads were washed three times

for 30 min at 4°C with buffer C (buffer B containing 0.1% (w/v) digitonin). Proteins bound to the sepharose beads were eluted with Tris/Tricine SDS–PAGE loading buffer lacking β-mercaptoethanol. β-Mercaptoethanol was added before samples were analysed by Tris/Tricine gradient SDS–PAGE (8–17.5%) (Schägger, 2006). Proteins were identified by peptide mass finger printing (CECAD mass spectrometry facility).

Affinity purification of protein complexes

Purified mitochondria (5 mg protein; CG214, CG591, CG593) harbouring C-terminally TAP-tagged Ups1 or Ups2 were solubilized as described above. The TAP-tag consisted of the calmodulin-binding peptide and protein A. After a clarifying spin, supernatant fractions were incubated with immunoglobulin G fast flow 6 beads (GE Healthcare) rotating over night at 4°C. Beads were washed twice with buffer C and once with 5 mM ammonium acetate pH 5.0. Bound proteins were eluted first with 0.5 M acetate pH 3.4 and second with Tris/Tricine SDS–PAGE loading buffer lacking β-mercaptoethanol. β-Mercaptoethanol was added before samples were analysed by Tris/Tricine SDS–PAGE (16%) and immunoblotting.

Metal chelating chromatography

Purified mitochondria harbouring the proteolytic inactive variant of Yme1^{E541Q} containing an N-terminal hexahistidine tag (Yme1(1–50)-6xHIS-Yme1(51–747)-E541Q) were subjected to Ni-NTA affinity chromatography. Mitochondria harbouring Yme1^{E541Q} lacking a hexahistidine tag served as a negative control. Crude mitochondria (40 mg of protein) were solubilized at a protein concentration of 4 mg/ml in 0.5% (w/v) dodecylmaltoside, 150 mM K-acetate pH 7.4, 30 mM Tris/HCl pH 7.4, 4 mM Mg-acetate, 1 × complete proteinase-inhibitor mix without EDTA (Roche), 1 mM PMSF, 20 mM imidazole/HCl pH 7.4, 10% glycerol. After a clarifying spin, the imidazole concentration of mitochondrial extracts was adjusted to 100 mM, before the sample was loaded onto Ni-NTA sepharose beads. Beads were washed with buffer containing 150 mM imidazole. Bound proteins were eluted with a linear imidazole gradient (100–750 mM). Yme1-containing eluate fractions were pooled, subjected to TCA precipitation (Tatsuta and Langer, 2007) and analysed by 7–20% (w/v) SDS–PAGE. Ups2 was detected in the eluate by peptide mass finger printing (CECAD mass spectrometry facility).

Protein import into mitochondria and degradation assays

UPS1 and *UPS2* were cloned into pGEM4, transcribed and translated in the presence of ^{35}S-methionine using reticulocyte lysate (Ambion, Promega). Radiolabelled proteins were imported into mitochondria at 25°C in the presence of dithiothreitol (5 mM) for the time points indicated essentially as described previously (Tatsuta and Langer, 2007). The import reaction was halted and non-imported proteins were degraded by proteinase K treatment (50 μg/ml, 15 min at 4°C) of the samples directly after import. Protease digestion was stopped by addition of PMSF (2 mM). Mitochondria were washed with SEM buffer containing protease inhibitor and analysed by Tris/Tricine gradient SDS–PAGE and autoradiography.

To assess the stability of newly imported Ups1 or Ups2, the import reaction was halted after 10 min at 25°C. After trypsin digestion (0.17 μg/μl, 15 min at 4°C) of non-imported proteins, protease digestion was stopped by addition of 1.3 μg/μl trypsin inhibitor. Mitochondria were washed twice in import buffer containing trypsin inhibitor and resuspended in import buffer supplemented with 2 mM ATP, 2 mM NADH, 10 mM creatine phosphate and 0.1 mg/ml creatine kinase, lacking dithiothreitol. Samples were incubated at 37°C for the indicated times to allow proteolysis to occur and subsequently analysed by SDS–PAGE and autoradiography.

Antibody production

A GST-Mdm35 fusion protein, Ups1 carrying an N-terminal hexahistidine peptide, and Ups2 containing an N-terminal extension built up of a hexahistidine peptide and ubiquitin were expressed in *Escherichia coli*. Inclusion bodies were purified and used to raise antibodies in rabbits.

Miscellaneous

Phospholipids were analysed by TLC and Psd1 activity was determined as described (Osman *et al*, 2009a).

Supplementary data

Supplementary data are available at *The EMBO Journal* Online (http://www.embojournal.org).

Acknowledgements

We thank Phat Vinh Dip for his contributions during the initial phase of this project and M Baker, T Tatsuta and T Wai for critical comments on the paper. We are grateful to T Lamkemeyer and the CECAD mass spectrometry unit for their support. This work was supported by grants from the Deutsche Forschungsgemeinschaft (SFB635) and the European Research Council to TL.

Conflict of interest

The authors declare that they have no conflict of interest.

References

Bione S, D'Adamo P, Maestrini E, Gedeon AK, Bolhuis PA, Toniolo D (1996) A novel X-linked gene, G4.5. is responsible for Barth syndrome. *Nat Genet* **12:** 385–389

Bogenhagen DF, Wang Y, Shen EL, Kobayashi R (2003) Protein components of mitochondrial DNA nucleoids in higher eukaryotes. *Mol Cell Proteomics* **2:** 1205–1216

Brachmann CB, Davies A, Cost GJ, Caputo E, Li J, Hieter P, Boeke JD (1998) Designer deletion strains derived from Saccharomyces cerevisiae S288C: a useful set of strains and plasmids for PCR-mediated gene disruption and other applications. *Yeast* **14:** 115–132

Chacinska A, Koehler CM, Milenkovic D, Lithgow T, Pfanner N (2009) Importing mitochondrial proteins: machineries and mechanisms. *Cell* **138:** 628–644

Choi SY, Gonzalvez F, Jenkins GM, Slomianny C, Chretien D, Arnoult D, Petit PX, Frohman MA (2007) Cardiolipin deficiency releases cytochrome c from the inner mitochondrial membrane and accelerates stimuli-elicited apoptosis. *Cell Death Differ* **14:** 597–606

Claypool SM, Oktay Y, Boontheung P, Loo JA, Koehler CM (2008) Cardiolipin defines the interactome of the major ADP/ATP carrier protein of the mitochondrial inner membrane. *J Cell Biol* **182:** 937–950

Daum G, Gasser SM, Schatz G (1982) Import of proteins into mitochondria. *J Biol Chem* **257:** 13075–13080

Dee CT, Moffat KG (2005) A novel family of mitochondrial proteins is represented by the Drosophila genes slmo, preli-like and real-time. *Dev Genes Evol* **215:** 248–254

DeVay RM, Dominguez-Ramirez L, Lackner LL, Hoppins S, Stahlberg H, Nunnari J (2009) Coassembly of Mgm1 isoforms requires cardiolipin and mediates mitochondrial inner membrane fusion. *J Cell Biol* **186:** 793–803

Dimmer KS, Fritz S, Fuchs F, Messerschmitt M, Weinbach N, Neupert W, Westermann B (2002) Genetic basis of mitochondrial function and morphology in Saccharomyces cerevisiae. *Mol Biol Cell* **13:** 847–853

Dunn CD, Tamura Y, Sesaki H, Jensen RE (2008) Mgr3p and Mgr1p are adaptors for the mitochondrial i-AAA protease complex. *Mol Biol Cell* **19:** 5387–5397

Gabriel K, Milenkovic D, Chacinska A, Muller J, Guiard B, Pfanner N, Meisinger C (2007) Novel mitochondrial intermembrane space proteins as substrates of the MIA import pathway. *J Mol Biol* **365:** 612–620

Gaigg B, Simbeni R, Hrastnik C, Paltauf F, Daum G (1995) Characterization of a microsomal subfraction associated with mitochondria of the yeast, Saccharomyces cerevisiae.

Involvement in synthesis and import of phospholipids into mitochondria. *Biochim Biophys Acta* **1234:** 214–220

Gebert N, Joshi AS, Kutik S, Becker T, McKenzie M, Guan XL, Mooga VP, Stroud DA, Kulkarni G, Wenk MR, Rehling P, Meisinger C, Ryan MT, Wiedemann N, Greenberg ML, Pfanner N (2009) Mitochondrial cardiolipin involved in outer-membrane protein biogenesis: implications for Barth syndrome. *Curr Biol* **19:** 2133–2139

Gohil VM, Thompson MN, Greenberg ML (2005) Synthetic lethal interaction of the mitochondrial phosphatidylethanolamine and cardiolipin biosynthetic pathways in Saccharomyces cerevisiae. *J Biol Chem* **280:** 35410–35416

Hoffmann B, Stockl A, Schlame M, Beyer K, Klingenberg M (1994) The reconstituted ADP/ATP carrier activity has an absolute requirement for cardiolipin as shown in cysteine mutants. *J Biol Chem* **269:** 1940–1944

Hoppins S, Lackner L, Nunnari J (2007) The machines that divide and fuse mitochondria. *Annu Rev Biochem* **76:** 751–780

Houtkooper RH, Turkenburg M, Poll-The BT, Karall D, Perez-Cerda C, Morrone A, Malvagia S, Wanders RJ, Kulik W, Vaz FM (2009) The enigmatic role of tafazzin in cardiolipin metabolism. *Biochim Biophys Acta* **1788:** 2003–2014

Houtkooper RH, Vaz FM (2008) Cardiolipin, the heart of mitochondrial metabolism. *Cell Mol Life Sci* **65:** 2493–2506

Kasashima K, Sumitani M, Satoh M, Endo H (2008) Human prohibitin 1 maintains the organization and stability of the mitochondrial nucleoids. *Exp Cell Res* **314:** 988–996

Lange C, Nett JH, Trumpower BL, Hunte C (2001) Specific roles of protein-phospholipid interactions in the yeast cytochrome bc1 complex structure. *EMBO J* **20:** 6591–6600

Leonhard K, Guiard B, Pellechia G, Tzagoloff A, Neupert W, Langer T (2000) Membrane protein degradation by AAA proteases in mitochondria: extraction of substrates from either membrane surface. *Mol Cell* **5:** 629–638

Leonhard K, Herrmann JM, Stuart RA, Mannhaupt G, Neupert W, Langer T (1996) AAA proteases with catalytic sites on opposite membrane surfaces comprise a proteolytic system for the ATP-dependent degradation of inner membrane proteins in mitochondria. *EMBO J* **15:** 4218–4229

Longen S, Bien M, Bihlmaier K, Kloeppel C, Kauff F, Hammermeister M, Westermann B, Herrmann JM, Riemer J (2009) Systematic analysis of the twin cx(9)c protein family. *J Mol Biol* **393:** 356–368

Merkwirth C, Dargazanli S, Tatsuta T, Geimer S, Lower B, Wunderlich FT, von Kleist-Retzow JC, Waisman A, Westermann B, Langer T (2008) Prohibitins control cell proliferation and apoptosis by regulating OPA1-dependent cristae morphogenesis in mitochondria. *Genes Dev* **22:** 476–488

Nebauer R, Schuiki I, Kulterer B, Trajanoski Z, Daum G (2007) The phosphatidylethanolamine level of yeast mitochondria is affected by the mitochondrial components Oxa1p and Yme1p. *FEBS J* **274:** 6180–6190

Neupert W, Herrmann JM (2007) Translocation of proteins into mitochondria. *Annu Rev Biochem* **76:** 723–749

Osman C, Haag M, Potting C, Rodenfels J, Dip PV, Wieland FT, Brugger B, Westermann B, Langer T (2009a) The genetic interactome of prohibitins: coordinated control of cardiolipin and phosphatidylethanolamine by conserved regulators in mitochondria. *J Cell Biol* **184:** 583–596

Osman C, Merkwirth C, Langer T (2009b) Prohibitins and the functional compartmentalization of mitochondrial membranes. *J Cell Sci* **122:** 3823–3830

Osman C, Wilmes C, Tatsuta T, Langer T (2007) Prohibitins interact genetically with Atp23, a novel processing peptidase and chaperone for the F_1F_O-ATP synthase. *Mol Biol Cell* **18:** 627–635

Riemer J, Bulleid N, Herrmann JM (2009) Disulfide formation in the ER and mitochondria: two solutions to a common process. *Science* **324:** 1284–1287

Schägger H (2006) Tricine-SDS-PAGE. *Nat Protoc* **1:** 16–22

Schlame M, Ren M (2006) Barth syndrome, a human disorder of cardiolipin metabolism. *FEBS Lett* **580:** 5450–5455

Schlame M, Ren M (2009) The role of cardiolipin in the structural organization of mitochondrial membranes. *Biochim Biophys Acta* **1788:** 2080–2083

Sesaki H, Dunn CD, Iijima M, Shepard KA, Yaffe MP, Machamer CE, Jensen RE (2006) Ups1p, a conserved intermembrane space protein, regulates mitochondrial shape and alternative topogenesis of Mgm1p. *J Cell Biol* **173:** 651–658

Sherman F (2002) Getting started with yeast. *Methods Enzymol* **350:** 3–41

Shinzawa-Itoh K, Aoyama H, Muramoto K, Terada H, Kurauchi T, Tadehara Y, Yamasaki A, Sugimura T, Kurono S, Tsujimoto K, Mizushima T, Yamashita E, Tsukihara T, Yoshikawa S (2007) Structures and physiological roles of 13 integral lipids of bovine heart cytochrome c oxidase. *EMBO J* **26:** 1713–1725

Tamura Y, Endo T, Iijima M, Sesaki H (2009) Ups1p and Ups2p antagonistically regulate cardiolipin metabolism in mitochondria. *J Cell Biol* **185:** 1029–1045

Tatsuta T, Langer T (2007) Studying proteolysis within mitochondria. *Methods Mol Biol* **372:** 343–360

Tatsuta T, Model K, Langer T (2005) Formation of membrane-bound ring complexes by prohibitins in mitochondria. *Mol Biol Cell* **16:** 248–259

Trotter PJ, Pedretti J, Voelker DR (1993) Phosphatidylserine decarboxylase from Saccharomyces cerevisiae. Isolation of mutants, cloning of the gene, and creation of a null allele. *J Biol Chem* **268:** 21416–21424

Weber ER, Hanekamp T, Thorsness PE (1996) Biochemical and functional analysis of the *YME1* gene product, an ATP and zinc-dependent mitochondrial protease from *S. cerevisiae*. *Mol Biol Cell* **7:** 307–317

Wenz T, Hielscher R, Hellwig P, Schägger H, Richers S, Hunte C (2009) Role of phospholipids in respiratory cytochrome bc(1) complex catalysis and supercomplex formation. *Biochim Biophys Acta* **1787:** 609–616

Wittig I, Schägger H (2009) Supramolecular organization of ATP synthase and respiratory chain in mitochondrial membranes. *Biochim Biophys Acta* **1787:** 672–680

Zeng X, Neupert W, Tzagoloff A (2007) The metalloprotease encoded by ATP23 has a dual function in processing and assembly of subunit 6 of mitochondrial ATPase. *Mol Biol Cell* **18:** 617–626

Zhong Q, Gohil VM, Ma L, Greenberg ML (2004) Absence of cardiolipin results in temperature sensitivity, respiratory defects, and mitochondrial DNA instability independent of pet56. *J Biol Chem* **279:** 32294–32300

